

PREPARATION AND PROPERTIES OF TITANIUM TRISULFIDE NANOPARTICLES

P. A. Poltarak^{1,2}, A. A. Poltarak^{1,2},
S. B. Artemkina^{1*}, T. Yu. Podlipskaya¹,
and V. E. Fedorov^{1,2}

UDC 546.824:549.32/.33

Stable colloidal dispersions with a 2 mM TiS_3 concentration (300 mg/l) are obtained by ultrasonic treatment of TiS_3 in acetonitrile and isopropyl alcohol and characterized by physicochemical methods. The electrical double layers for the particles in dispersions are estimated from the measured ζ -potentials, and the energies of interparticle interactions are calculated based on the Derjaguin–Landau–Verwey–Overbeek theory. The structural and spectroscopic identity of the particles and crystalline TiS_3 is demonstrated for the solid phases obtained from the dispersions.

DOI: 10.1134/S0022476617050250

Keywords: layered compounds, titanium trisulfide, colloidal dispersion, ultrasonic dispersing, titanium trisulfide nanoparticles, photon correlation spectroscopy, hydrodynamic diameter, transmission electron microscopy.

INTRODUCTION

The first publications on graphene [1] and exfoliation of transition metal dichalcogenides [2] gave rise to considerable interest in the study of other layered materials, particularly nanosized samples. One of the promising ways to obtain nanoparticles is the dispersing of compact crystalline samples with the formation of colloidal dispersions. This approach has been successfully applied to the compounds with layered structures, for example, multilayered graphene materials, transition metal dichalcogenides MQ_2 ($\text{M} = \text{Ti}, \text{Zr}, \text{Hf}; \text{V}, \text{Nb}, \text{Ta}; \text{Mo}, \text{W}; \text{Q} = \text{S}, \text{Se}$), and others. In our work we consider another large family of transition metal trichalcogenides, which can be structurally attributed to layered systems. According to the structural and spectroscopic data, trichalcogenides MQ_3 ($\text{M} = \text{Ti}, \text{Zr}, \text{Hf}, \text{Nb}, \text{Ta}, \text{U}; \text{Q} = \text{S}, \text{Se}, \text{Te}$) can be described by an ionic model $\text{M}^{4+}(\text{Q}_2)^{2-}\text{Q}^{2-}$ [3] containing chalcogenide ions Q^{2-} and dichalcogenide groups $(\text{Q}_2)^{2-}$. Although the $\{\text{MQ}_{6/2}\}$ prism is a basic structural unit for MQ_2 and MQ_3 , transition metal trichalcogenides have more complex crystal structures. Non-equivalence of chalcogen atoms in MQ_3 results in the formation of distorted (wedge-shaped) prisms, where shortened Q–Q bonds point at the dichalcogenide groups $(\text{Q}_2)^{2-}$. These prisms with M atoms inside (located close to the center of the prisms) share triangular bases and form infinite columns oriented along the b direction (Fig. 1a). Due to short M...Q contacts between the neighboring columns, polymer layers form whose surfaces are formed by dichalcogenide groups $(\text{Q}_2)^{2-}$ (Fig. 1b). Therefore, transition metal trichalcogenides MQ_3 can be considered as layered compounds together with dichalcogenides MQ_2 .

¹Nikolaev Institute of Inorganic Chemistry, Siberian Branch, Russian Academy of Sciences, Novosibirsk, Russia;
^{*}artem@niic.nsc.ru. ²Novosibirsk National Research State University, Russia. Translated from *Zhurnal Strukturnoi Khimii*, Vol. 58, No. 5, pp. 1072–1077, June–July, 2017. Original article submitted December 28, 2016.

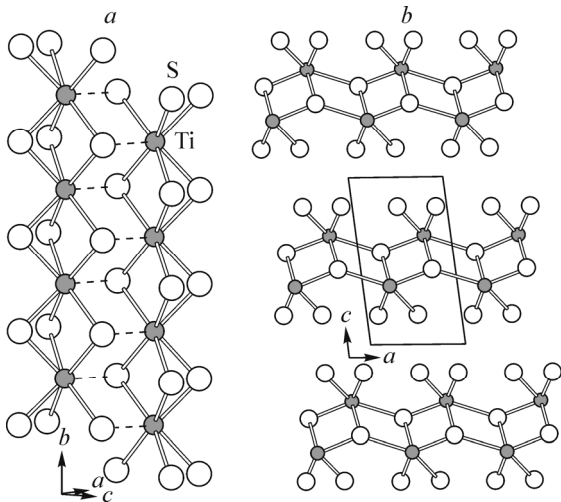


Fig. 1. Two wedge-shaped columns (*a*) and the packing of polymer layers in the crystal structure of TiS_3 (*b*).

The crystal structure of monoclinic TiS_3 belongs to the ZrSe_3 structure type, which has one type of wedge-shaped columns [4, 5]. In the approximation of the ionic model, titanium in TiS_3 has the d^0 electronic configuration, and this compound is a diamagnetic semiconductor. The quantum chemical modeling of the electronic structure of TiS_3 [6] gives the band gap in a range of 0.48–2.17 eV; the calculated optical absorption spectra show the onset of light absorption within 0.9–1.5 eV suggesting its possible use in photovoltaics and photocatalysis.

By optical methods it is established that on passing from crystalline TiS_3 to nanolayers the second direct optical transition appears: $E_{g1} = 1.0 \pm 0.1$ eV and $E_{g2} = 1.4 \pm 0.1$ eV [7]. The investigation of TiS_3 nanoribbons revealed interesting physical properties. A thin TiS_3 particle (with a thickness of several crystallographic layers) exhibits planar anisotropy of the electroconductivity. Under room conditions the anisotropy is 2.1 [8] (for example, cf. with 1.8 for black phosphorus [9]). In another research, TiS_3 nanoribbons were used as an anode in the hydrogen reaction. The efficiency of hydrogen photogeneration was 7% [10]. For these experiments TiS_3 nanocrystals were used.

We have recently reported the studies on obtaining NbS_3 , NbSe_3 , TaS_3 nanoparticles [11–13]. Indeed, during ultrasonic treatment trichalcogenides, which are deemed to have layered structures, exfoliated and formed thin nanoparticles with a diameter of hundreds of nanometers and a thickness of 2–20 nm. In this work, with the aim to prepare TiS_3 powders and other materials containing TiS_3 with large surface areas, we obtained colloidal dispersions of TiS_3 in liquid media under ultrasonic effect. The TiS_3 particles in these colloidal dispersions and some properties of these colloidal dispersions are discussed.

EXPERIMENTAL

Methods and equipment. Powder X-ray diffraction (XRD) patterns were recorded on a Philips PW 1830/1710 diffractometer (CuK_{α} radiation, graphite monochromator; silicon slab was the external standard). Raman spectra were recorded on a Triplemate spectrometer (laser wavelength of 488 nm). The electronic absorption spectra (EAS) were recorded on an Agilent Cary 60 spectrometer in a wavelength range from 200 nm to 1100 nm.

Particle sizes were measured by photon correlation spectroscopy (PCS) on a NanoBrook Omni spectrometer (Brookhaven, USA) in glass cuvettes (1 cm) at 20 °C. The photon accumulation time per measurement was 10 s. The solid state laser power with an emission wavelength of 640 nm was 35 mW; a detector was located at an angle of 90° to the laser radiation source. The medium z-averaged (over intensities) hydrodynamic diameter D_h was calculated by the Stokes–Einstein formula [14] for spherical particles as a mean of 25–30 measurements. The method error did not exceed 5%.

The electrophoretic mobility of particles and the conductivity of colloidal dispersions were measured on a Zetasizer Nano ZS device (Malvern Instr.). Three parallel measurements were taken for each dispersion. Electrokinetic potentials were calculated by the Smoluchowski formula.

Transmission electron microscopy (TEM) images of the particles were obtained on a JEM 4000EX microscope with an accelerating voltage of 400 kV. The dispersing was carried out in Sapfir ultrasonic baths (power 130 W). The resulting dispersions were centrifuged on an Eppendorf 5430 centrifuge in 50 ml tubes.

Synthesis of TiS₃. 6.991 g (0.2181 mol) of crystalline sulfur and 3.323 g (0.06942 mol) of titanium powder were placed in a quartz ampoule (volume 45 ml). A sulfur excess is required to prevent the decomposition of titanium trisulfide into disulfide and sulfur. The ampoule was evacuated, sealed, and placed in a furnace. The synthesis was performed at a temperature of 500 °C for 150 h. The resulting product was washed from the sulfur excess with toluene in a Soxhlet extractor.

Preparation of colloidal dispersions of TiS₃. Titanium trisulfide TiS₃ (100 mg) was placed in 100 ml of an organic medium and subjected to ultrasonic treatment at 60% of the bath power for 40 h. Acetonitrile (CH₃CN), ethanol, dimethyl formamide (DMF), isopropanol (*i*-PrOH), *n*-methylpyrrolidone, and dimethyl sulfoxide (DMSO) were used as the dispersion media. After ultrasonic treatment all colloidal solutions were centrifuged (2000 rps, 500 g, 10 min). Then we dealt with dispersions in acetonitrile and isopropanol because they did not coagulate for at least a week.

Determination of the concentration of colloidal dispersions. An aliquot of the dispersion was passed through a Whatman Anodisc filter (pore size of 0.02 µm). The obtained filter with a layer of the solid phase from the colloidal dispersion was dried in a drying furnace at 80 °C for 2 h. The TiS₃ content in the solutions was calculated from the mass difference before and after filtering.

RESULTS AND DISCUSSION

Initial TiS₃. TiS₃ prepared is a dark gray crystalline solid product resembling a sponge due to a large number of needle-shaped crystals. All reflections observed in the powder XRD pattern belong to the structure of titanium trisulfide determined previously in [5] (ICSD No 42-072); no other reflections were found. The lines in the Raman spectrum correspond to the vibrational modes of the TiS₃ lattice [15]. Thus, it can be concluded that the product synthesized is pure titanium trisulfide.

Colloidal dispersions of TiS₃. Ultrasonication experiments on TiS₃ in different media showed that TiS₃ was well dispersed in acetonitrile and isopropanol forming stable (over 7 days) gray dispersions. The dispersions in acetonitrile and isopropanol contained 390 mg/l (2.7 mM TiS₃ formula units) and 260 mg/l (1.8 mM TiS₃) respectively. Ultrasonic treatment of TiS₃ in other media (DMSO, DMF, ethanol, and *n*-methylpyrrolidone) did not result in the formation of stable colloidal dispersions.

In EAS (Fig. 2) a characteristic increase in the degree of absorption with decreasing wavelength explained by Rayleigh scattering on colloidal particles can be observed. EAS of the TiS₃ colloidal dispersions in general repeat each other; the absorption bands are at 950 nm, 640 nm, 400 nm, and 280 nm.

In the TEM images (Fig. 3a) it is seen that the main part of the particles are elongated plates whose lateral dimensions strongly vary in a range from tens of nanometers to units of microns. Electron diffraction on one TiS₃ particle (Fig. 3b; the particle image is shown in the inset) was indexed in the space group P2₁/m; the extinctions characteristic of this symmetry group were observed in the image (the observability conditions of reflections 0k0: $k = 2n$). Hence, we can conclude that the particles in colloidal solutions are crystalline. The TEM images indicate the presence of an amorphized layer on the surface of TiS₃ particles; for the particles in the isopropanol dispersion its thickness is 5-10 nm.

Results of the PCS study of the particle size in TiS₃ dispersions and their electrokinetic potential are given in Table 1. The obtained data were used to estimate the stability of TiS₃ dispersions in acetonitrile and isopropyl alcohol following the Derjaguin–Landau–Verwey–Overbeek theory (DLVO theory [16]).

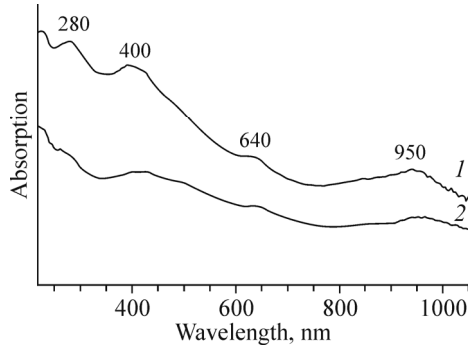


Fig. 2. Electronic absorption spectra of the TiS_3 colloidal dispersions in acetonitrile (1) and isopropanol (2).

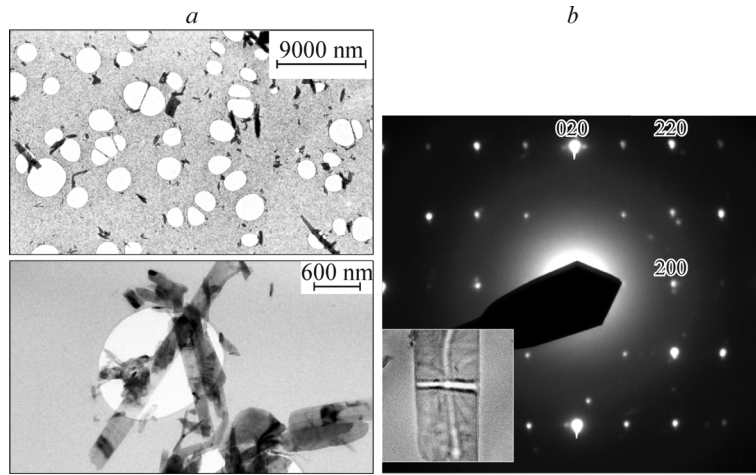


Fig. 3. Images (TEM) of the TiS_3 particles obtained by ultrasonic dispersing in isopropanol (a). Electron diffraction on the TiS_3 particle (b) and its image in the inset.

TABLE 1. Average Hydrodynamic Diameters (D_h), Electrokinetic Potentials (ζ), Electroconductivity (σ) and the Calculated Electrical Double Layers (δ) of the Particles in the TiS_3 Colloidal Dispersions

Medium (ϵ at 25 °C)	D_h , nm	ζ , mV	σ , mS/cm	C , mol/l	δ , nm	Observed stability
CH_3CN (38.0)	174	-30.1	0.01292	$1.10 \cdot 10^{-4}$	20.2	Good
$i\text{PrOH}$ (18.3)	234	-60.0	0.00679	$5.80 \cdot 10^{-5}$	19.3	Good

According to the DLVO theory, it is possible to calculate the potential barrier height (or the potential well depth) and estimate the stability of the obtained dispersions from the electrokinetic potential, electroconductivity, particle sizes and shapes. As evident from Table 1, in both solvents the nanoparticles carry a negative surface charge, but its origin is not known.

The interparticle interactions were calculated using the DLVO theory for spherical particles with the sizes equal to the effective hydrodynamic diameters. The formulas required for the calculations and the assumptions made were taken from our previous study of NbS_2 particles [11].

Fig. 4 shows the calculated electrostatic, van der Waals, and total energies of interparticle interactions of TiS_3 particles depending on the distance l between them for the dispersions in acetonitrile and isopropyl alcohol. For both systems, large values of potential barrier height were obtained: $17kT$ ($l_{\max} = 6$ nm) for the dispersion in acetonitrile and $50kT$

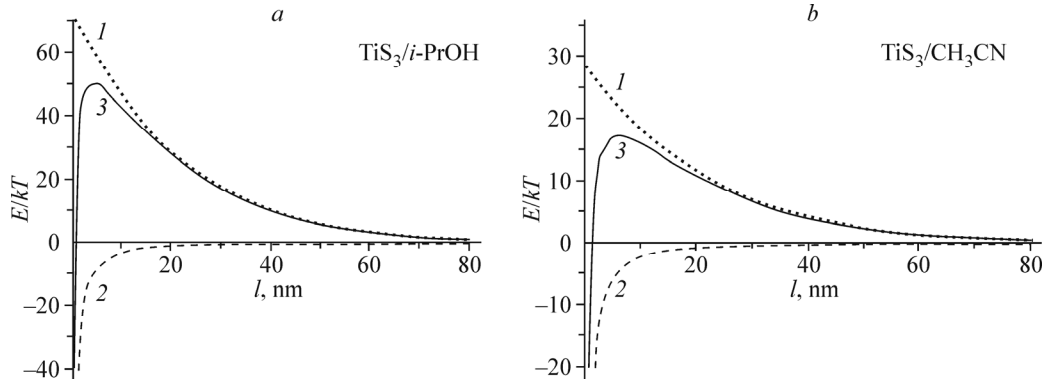


Fig. 4. Electrostatic (I), van der Waals (2), and total (3) energies of interparticle interactions depending on the distance l between the spherical particles for the TiS_3 dispersions in isopropyl alcohol (a) and acetonitrile (b).

($l_{\max} = 5 \text{ nm}$) for the dispersion in isopropanol. Note that the DLVO theory estimates agree well with the visually observed stability of the dispersions.

The precipitates from the colloidal dispersions of TiS_3 were analyzed using powder XRD and Raman scattering. All reflections observed (Fig. 5) belong to titanium trisulfide phases. For the precipitate obtained from the isopropanol dispersion an increase in the $00l$ reflection intensity was observed as compared to other reflections, which can be explained by a high degree of texturization since the particles in the $00l$ crystallographic direction are mainly oriented parallel to the filter plane. This effect was not observed for the acetonitrile dispersion.

The positions of vibrational bands in the Raman spectra of dispersed TiS_3 correspond to the vibrational bands of crystalline samples, the appearance of new bands or a change in the shape of the existing ones being not observed. The vibrational bands in the spectra are in the following positions (in parentheses the data are given from [15]): A_g 174 (175 cm^{-1}), A_g 296 (300 cm^{-1}), A_g, B_g 367 (366 cm^{-1} and 370 nm^{-1}), A_g 554 (557 cm^{-1}). The powder XRD and Raman spectral data allow us to conclude that during the ultrasonic dispersing in acetonitrile and isopropanol the TiS_3 structure remains unchanged.

Thus, the work shows that TiS_3 particles in the form of micronanoribbons can be obtained by ultrasonic treatment of crystalline TiS_3 in acetonitrile and isopropanol, with the TiS_3 content in the colloidal dispersion being $\approx 2 \text{ mM}$. The TiS_3

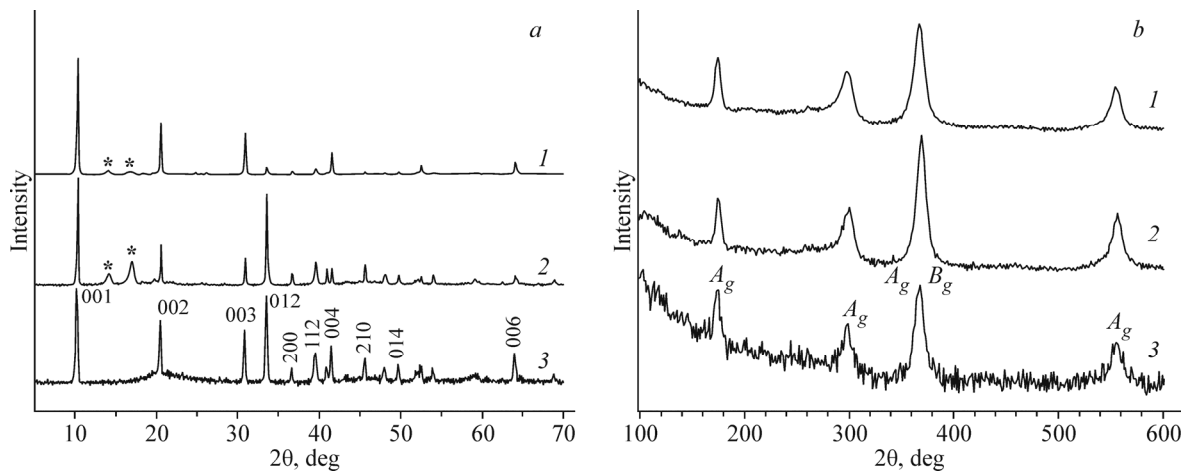


Fig. 5. Powder XRD patterns of the particles deposited on the filter from the TiS_3 colloidal solutions in isopropanol (1) and acetonitrile (2), and of crystalline TiS_3 (3). The filter reflections are denoted by asterisks (a). The Raman spectra of the TiS_3 precipitates from the colloidal dispersions in isopropanol (1) and acetonitrile (2) and of initial TiS_3 (3) (b).

dispersions are the matrices with a large surface area and are stable for more than one week. This can be useful for the preparation of different composites for photocatalysis and other applications.

The work was supported by RFBR (RFBR grant No. 16-33-00577mol_a).

The authors are grateful to D-r I. A. Pyshnaya (Institute of Chemical Biology and Fundamental Medicine, Siberian Branch of the RAS) for measurement of the electrokinetic potentials.

REFERENCES

1. J. N. Coleman, *Acc. Chem. Res.*, **46**, No. 1, 14-22 (2013).
2. V. Nicolosi, M. Chhowalla, M. G. Kanatzidis, et al., *Science*, **340**, 1226419 (2013).
3. V. E. Fedorov, *Chalcogenides of High-Melting Transition Metals. Quasi-One-Dimensional Compounds* [in Russian], Nauka, Novosibirsk (1988).
4. L. Brattas and A. Kjekshus, *Acta Chem. Scandin.*, **26**, No. 9, 3441-3449 (1972).
5. S. Furuseth, L. Brattas, and A. Kjekshus, *Acta Chem. Scandin.*, **A29**, No. 6, 623-631 (1975).
6. M. Abdulsalam and D. P. Joubert, *Phys. Status Solidi B*, **253**, No. 5, 868-874 (2016).
7. I. J. Ferrer, J. R. Ares, J. M. Clamagirand, et al., *Thin Solid Films*, **535**, 398-401 (2013).
8. J. Island, R. Biele, M. Barawi, et al., *Sci. Rep.*, **6**, 22214 (2016).
9. F. Xia, H. Wang, and Y. Jia, *Nature Commun.*, **5**, 4458 (2014).
10. M. Barawi, E. Flores, I. J. Ferrer, et al., *J. Mater. Chem. A*, **3**, No. 15, 7959-7965 (2015).
11. S. B. Artemkina, T. Y. Podlipskaya, A. I. Bulavchenko, et al., *Colloids and Surfaces A: Physicochem. Engineer. Aspects*, **461**, 30-39 (2014).
12. V. E. Fedorov, S. B. Artemkina, N. G. Naumov, et al., *J. Mater. Chem. C*, **2**, No. 28, 5479-5486 (2014).
13. P. A. Poltorak, S. B. Artemkina, A. I. Bulavchenko, et al., *Russ. Chem. Bull.*, **64**, No. 8, 1850-1856 (2015).
14. G. D. J. Phillips, *Analyt. Chem.*, **62**, No. 20, 1049-1057 (1990).
15. P. Gard, F. Cruege, C. Sourisseau, and O. Gorochov, *J. Raman Spectrosc.*, **17**, 283-288 (1986).
16. B. V. Derjaguin, N. V. Churaev, and V. M. Muller, *The Derjaguin Landau Verwey Overbeek (DLVO) Theory of Stability of Lyophobic Colloids*, Springer, New York (1987), pp. 293-310.